nature communications

Article

https://doi.org/10.1038/s41467-024-54383-y

DUSP6 regulates Notch1 signalling in colorectal cancer

Received: 16 May 2023

Accepted: 8 November 2024

Published online: 21 November 2024

Check for updates

Chin Wen Png[1,2,3,8], Madhushanee Weerasooriya[1,2,3,8], Heng Li[1,2,3,8], Xiaowen Hou[1,2,3], Fiona Yayuan Teo[1,2,3], Shiying Huang[1,2,3], Zheng Ser[4], Franklin Yau Kok Weng[1,2,3], Malini Rethnam[5,6], Gloryn Chia[5,6], Radoslaw M. Sobota[4], Choon Seng Chong[7], Ker-Kan Tan[7] & Yongliang Zhang[1,2,3]

Notch1 plays various roles in cancer development, and Notch1-induced transactivation is controlled by phosphorylation of its cleaved intracellular domain. However, it is unclear whether there are phosphatases capable of dephosphorylating the cleaved Notch1 transmembrane/intracellular region (NTM) to regulate its function. Here, we show that DUSP6 can function as a phosphatase for Notch1, thereby regulating NTM stability and transcriptional activity, thus influencing colorectal cancer (CRC) development. In human CRC cells, elevated DUSP6 expression correlates with increased NTM levels, leading to enhanced CRC cell proliferation both in vitro and in vivo. High tumoral DUSP6 protein expression is associated with poorer overall CRC patient survival. In mice, DUSP6 deficiency results in reduced CRC development. Mechanistically, DUSP6 dephosphorylates phospho-Y2116, which in turn reduces NTM ubiquitination, leading to increased NTM stability and transcriptional activity. As a result, the expression of Notch1-targeted proliferation genes is increased to promote tumour cell growth.

Pathogenesis of colorectal cancer (CRC) is multifaceted, involving dysregulation of multiple cellular signalling pathways that control intestinal epithelial cell proliferation, apoptosis and survival. Among these pathways, the mitogen-activated protein kinases (MAPKs) pathways, particularly the extracellular signal-regulated kinase 1/2 (ERK1/2) signalling, have been identified to be critical for the development of CRC. Dysregulation of ERK1/2 in cancer could be due to the alteration of various upstream regulators, leading to constitutive activation of ERK1/2 and resulting in the overexpression of target genes involved in tumorigenesis. For example, hyperactivating mutations along the EGFR-Ras-Raf-MEK-ERK1/2 signalling pathway that occurs in up to 45% of all CRC cases are associated with increased tumour cell growth, cancer progression and drug resistance[1]. Therefore, therapeutics that target components of the EGFR-Ras-Raf-MEK-ERK1/2 pathway were developed to limit ERK1/2 activation. On the other hand, others have shown that treatment with chemotherapeutics such as 5-FU and oxaliplatin could increase the activation of p38 and JNK MAPKs that, in turn, influence the stress responses and tumour cell apoptosis[2,3].

Among the various intrinsic factors that control MAPKs activities, dual-specificity protein phosphatases (DUSPs, also known as MAPK

[1]Department of Microbiology and Immunology, Yong Loo Lin School of Medicine, National University of Singapore, Singapore 117545, Singapore. [2]NUSMED Immunology Translational Research Programme, Yong Loo Lin School of Medicine, National University of Singapore, Singapore 117456, Singapore. [3]Immunology Programme, Life Science Institute, National University of Singapore, Singapore 117456, Singapore. [4]Functional Proteomics Laboratory, Sing-Mass National Laboratory, Institute of Molecular and Cell Biology (IMCB), Agency for Science, Technology and Research (A*STAR), Singapore 138673, Singapore. [5]Department of Pharmacy, Faculty of Science, National University of Singapore, Singapore 117597, Singapore. [6]Institute for Health Innovation & Technology (iHealthtech), National University of Singapore, Singapore 117597, Singapore. [7]Department of Surgery, Yong Loo Lin School of Medicine, National University of Singapore, Singapore 119228, Singapore. [8]These authors contributed equally: Chin Wen Png, Madhushanee Weerasooriya, Heng Li. e-mail: miczy@nus.edu.sg

phosphatases) are known as the major negative regulators of MAPKs[4]. At the same time, DUSPs are also regulated by MAPKs in a feedback loop system, operating alongside other post-translational modification mechanisms[5,6]. The complex regulation of DUSPs have contributed to its diverse roles in cancer pathogenesis. Studies have attributed DUSPs with opposing roles as oncogenes or tumour suppressors, dependent on the type of tumours and conditions. One such phosphatase is DUSP6 which has high substrate specificity for ERK1/2[7]. DUSP6 was shown to act as a tumour suppressor in lung cancer[8], nasopharyngeal carcinoma[9] and melanoma cancer[10] by inhibiting ERK1/2 activation. On the other hand, others have shown that DUSP6 expression could be pro-tumorigenic, and has been implicated in the development of gastric cancer[11], cervical cancer[12], ovarian cancer[13] and glioblastomas[14]. However, the mechanisms underlying the differential function of DUSP6 in various types of cancers are unclear. Particularly, the pathogenic role of DUSP6 in CRC remains undefined. Nevertheless, studies have proposed that DUSP6 may contribute to the function of other proteins in CRC. For example, protein kinase N2 (PKN2), a member of a subfamily of protein kinase C, was found to inhibit IL-4 and IL-10 expression in CRC cell lines such as HCT116, thereby inhibiting macrophage M2 polarisation in CRC development[15]. Interestingly, PKN2 was found to interact with DUSP6 that could inhibit ERK1/2 phosphorylation. However, it was also found that PKN2 inhibits the binding of transcriptional factors, including Elk-1 and CREB, to the promoters of IL-4/IL-10, thereby inhibiting their transcription. Hence, the significance of DUSP6 in PKN2-mediated IL-4/IL-10 expression and M2 macrophage polarisation in CRC remains unclear. Similarly, the role of placenta-specific-8 (PLAC8) in unconventional ERK2-dependent colorectal cancer cell epithelial-to-mesenchymal transition (EMT) has been linked with DUSP6[16]. PLAC8 could bind to DUSP6 and somehow downregulate its phosphatase activity, thereby enhancing ERK2 phosphorylation. In addition, the function of immunoglobulin-like domain protein 3 (LRIG3) in the regulation of Slug-dependent EMT was also associated with its interaction with DUSP6[17]. It was shown that knockout of LRIG3 in CRC cell line SW480 resulted in increased ERK1/2 activation and Slug expression. The negative correlation between LRIG3 and Slug expression was likely due to the interaction of LRIG3 with both ERK1/2 and DUSP6. It was speculated that LRIG3 inhibits ERK1/2 activation through DUSP6, thereby inhibiting Slug expression and CRC EMT. While these studies suggest an association between DUSP6 and CRC pathogenesis, the specific involvement and regulatory function of DUSP6 remain unclear.

Besides EGFR, activation of other transmembrane molecules, such as Notch, plays a pivotal role in cellular development, cell growth, and cell fate determination. Consequently, aberrant Notch signalling is closely linked to tumorigenesis[18,19]. In fact, Notch is implicated in various hallmarks of cancer. Notch1 is one of the four Notch receptors expressed in mammalian cells. Mutations in the *NOTCH1* gene play key roles in the progression of human malignancies[20]. *NOTCH1* mutations have been reported to account for 4.48% of all cancers, with colon adenocarcinoma having the highest prevalence (https://www.mycancergenome.org/). Additionally, *NOTCH1* mutations were found in 8.37% of all cases of CRC based on data from the National Cancer Institute Genomic Data Common Portal (https://portal.gdc.cancer.gov/). Other studies have also shown that increased Notch1 activation is associated with a poorer prognosis for patients.[21,22]. Moreover, activation of Notch1 has been demonstrated to induce EMT, often contributing to metastatic CRC[23]. Activation of Notch1 is initiated by binding to its ligands, Delta-like proteins 1 and 3, or Jagged 1 and 2. This is followed by a cascade of proteolytic cleavages to release the Notch intracellular domain (NICD) which translocates into the nucleus for transcription of proliferation-associated genes such as c-Myc. Phosphorylation of NICD, which regulates its stability, is a key process that determines its biological activity. While phosphorylation of the cleaved NICD by corresponding kinases is known to modulate biological activity, the regulation by phosphatases has remained unexplored.

In this study, we show that high DUSP6 protein expression in tumours correlate with high cleaved Notch1 transmembrane/intracellular domain (NTM), and is associated with poorer overall survival in human CRC. Mechanistically, DUSP6 is a Notch1 phosphatase that regulates NTM level to promote CRC cell proliferation and hence is pro-tumourigenic in CRC.

Results

DUSP6 promotes cell growth and migration while suppressing the activation of MAPKs in CRC cells

To examine the regulatory function of DUSP6 in CRC cells, we generated DUSP6 overexpressing Caco2 cells (Caco2 DUSP6 OE) and DUSP6 knockout DLD1 cells (DLD1 DUSP6 KO). To note, Caco2 cells expressed a lower level of DUSP6 compared to DLD1 cells (Supplementary Fig. S1a). It was observed that Caco2 DUSP6 OE cells exhibited increased proliferation after 48 h in standard culture condition, and the growth continued to be significantly higher after 72 h of culture compared to Caco2 vector control cells (Fig. 1a, left panel). Similarly, increased growth was observed when Caco2 DUSP6 OE cells were cultured in a medium containing EGF (Fig. 1a, right panel). When cells were cultured in a serum-free medium, Caco2 DUSP6 OE cells also exhibited increased proliferation after 48 and 72 h with or without EGF (Supplementary Fig. S1b). In contrast, loss of DUSP6 in DLD1 resulted in a significant reduction in cell growth after 48 and 72 h of culture with or without EGF treatment in both standard and serum-free culture conditions (Fig. 1b and Supplementary Fig. S1c). Results from the wound healing assay demonstrated that Caco2 DUSP6 OE cells migrated 60% faster compared to the control (Fig. 1c), whereas migration was reduced in DLD1 DUSP6 KO cells by 60% compared to control cells. These results demonstrated that CRC cell migration was also positively regulated by DUSP6. The differences in cell migration are independent of cellular proliferation since cells were pre-treated with mitomycin-c to inhibit cell growth. Additionally, based on previous proliferation data, no significant differences in proliferation were observed at the 24-hour timepoint (Fig. 1a). To verify the role of DUSP6 in promoting CRC growth, a full-length DUSP6 cDNA containing plasmid was transfected into DUSP6 KO DLD1 cells to rescue its expression (Fig. 1e). Measurement of cell proliferation showed that the expression of DUSP6 rescued the reduced proliferation in DUSP6 KO DLD1 cells with or without EGF (Fig. 1f). Hence, it is evident that DUSP6 positively regulates CRC cell growth and migration.

DUSP6 has been shown to mainly target ERK1/2[24], a MAPK that plays an important role in controlling mitogenic signals for cell survival and proliferation. We, therefore, examined the effect of DUSP6 in the activation of MAPKs in both Caco2 DUSP6 OE and DLD1 DUSP6 KO cells in response to EGF which would activate the EGFR-Ras-Raf-MEK-ERK1/2 pathway. It was found that overexpression of DUSP6 in Caco2 cells resulted in reduced activation of ERK1/2, p38 and JNK, whereas knockout of this molecule in DLD1 cells increased their activation (Fig. 2a and Supplementary Figs. S2, S3). Interestingly, the expression of proliferation-associated genes, COX2 and c-MYC, was increased in Caco2 DUSP6 OE cells, particularly after EGF treatment for 9 hours, whereas reduced expression of COX2 and c-MYC was observed in DLD1 DUSP6 KO cells. The suppressive function of DUSP6 against the activation of MAPKs was further confirmed using Caco2 DUSP6 KO cells. Consistent with the observation in DLD1 DUSP6 KO, loss of DUSP6 in Caco2 cells resulted in increased phosphorylation of ERK, p38 and JNK, as well as reduced expression of COX2 and c-MYC in response to EGF treatment (Supplementary Fig. S4).

While the changes in proliferation profile were in accordance with the levels of COX2 and c-MYC in both DUSP6 OE and KO cell lines, this was surprising when compared to the alterations in MAPKs activity, particularly pERK1/2, which is often reported to be positively

https://doi.org/10.1038/s41467-024-54383-y

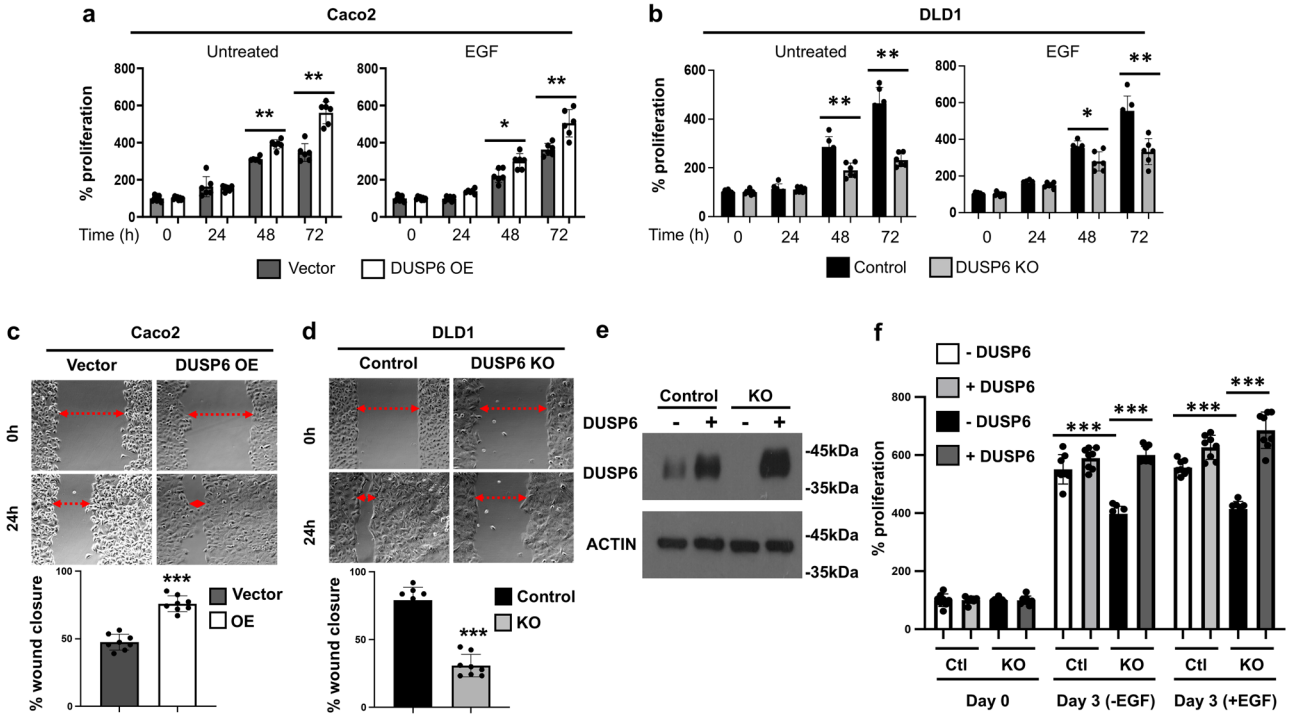

Fig. 1 | DUSP6 positively regulates cellular proliferation and migration in CRC cells in vitro. a, **b** Bar charts show the effect of DUSP6 expression on the rate of cell growth in Caco2 and DLD1 CRC cells with or without EGF treatment ($n = 6$ biologically independent samples). **c**, **d** Representative micrographs showing migration of Caco2 or DLD1 cells in wound healing assay. Bar charts under each micrograph panel show the percentage of wound closure/migration of cells compared to Time 0. Arrows denote the distance of each "wound" at the start of the experiment (Time = 0 h) and at the endpoint (Time = 24 h). **e** Western blot analysis of DUSP6 in vector and DUSP6 KO DLD1 cells transfected with a full-length cDNA of *DUSP6*. **f** Cell proliferation of DLD1 KO cells with or without DUSP6 overexpression was determined on Day 3 with or without EGF treatment. *, **, and *** denote $P < 0.05$, $P < 0.01$, and $P < 0.001$, respectively (two-tailed, nonparametric, Mann–Whitney test). Error bars = mean ± standard deviations. **c**, **d** and **f** ($n = 8$ biologically independent samples). Source data are provided as a Source Data file.

correlated with proliferation[13]. This suggests that alternative mechanisms and factors regulated by DUSP6 contribute to the proliferation profile observed in both Caco2 DUSP6 OE and DLD1 DUSP6 KO cells.

DUSP6 positively regulates cleaved Notch1 level and CRC cell growth in vivo

In CRC, various proliferation-associated genes and signalling molecules are upregulated in tumours. This includes Notch1 which was reported to be associated with poorer prognosis of CRC patients[22]. As a transmembrane receptor protein, activation of Notch1 requires proteolytic cleavage by gamma-secretase (γ-secretase) to release the cleaved Notch1 intracellular region for transcriptional activation of target proliferation-associated genes or cooperation with other cellular factors[18,25]. Changes in the amount of cleaved Notch1 would influence cellular proliferation in a positive manner. To examine the potential regulation of Notch1 by DUSP6, the levels of cleaved Notch1 intracellular region in Caco2 and DLD1 cells, which are Notch1 wildtype[26], were examined. To note, the antibody used to examine the cleaved Notch1 intracellular region by Western blot analysis in this study detects the entire Notch1 intracellular domain, as well as a short extracellular juxtamembrane peptide and a transmembrane sequence with a molecular weight of 120 kDa, which is referred to as 'NTM' (see Supplementary Methods).

A higher level of NTM was observed in parental DLD1 cells, which express higher DUSP6, compared to that of Caco2 cells, which express a lower level of DUSP6 (Supplementary Fig. S1). The overexpression of DUSP6 in Caco2 cells led to elevated NTM levels, whereas knockout of DUSP6 resulted in reduced levels of NTM in DLD1 cells compared to their respective control cells (Fig. 2b and Supplementary Figs. S3, S4). These results suggest that the expression of DUSP6 is positively associated with the NTM level. On the other hand, the expression of key components of γ-secretase, including Presenilin 1 (PSEN1), Presenilin 2 (PSEN2), PEN2 and Nicastrin (NCSTN) were comparable in both DUSP6 OE and DUSP6 KO cells compared to their respective controls after EGF treatment. However, endogenous γ-secretase activity was found to be increased in Caco2 DUSP6 OE cells by 80% (Fig. 2c). Contradictorily, γ-secretase activity was reduced by 48% in DLD1 DUSP6 KO cells compared to that in control cells.

It has been shown that ERK1/2 could phosphorylate PSEN1, thereby regulating the activity of γ-secretase[27]. To test if DUSP6 regulates cleaved Notch1 level through ERK1/2, DUSP6 KO DLD1 and control cells were treated with an ERK-specific inhibitor to examine the levels of NTM. Interestingly, ERK inhibition did not affect the levels of NTM in both vector and DUSP6 KO cells (Fig. 2d), despite the differences in the level of γ-secretase activity (Fig. 2e). Both vector and KO cells exhibited reduced proliferation upon ERK inhibition (Fig. 2f), but the proliferation of KO cells remained significantly lower compared to vector cells.

Next, Caco2 and DLD1 xenograft models were employed to test the function of DUSP6 in CRC cell growth in vivo. Increased expression of DUSP6 in Caco2 cells led to the development of larger tumour xenografts, which were 3.3-fold heavier than the xenografts developed from Caco2 vector control cells (Fig. 3a). In contrast, loss of DUSP6 in Caco2 cells resulted in the formation of xenografts that were 8.5-fold smaller than control cells (Supplementary Fig. S5). Immunostaining of the xenografts showed significant increases in both Ki67 and cleaved Notch1 levels in Caco2 DUSP6 OE tumour xenografts compared to control (Fig. 3b, c). Consistent with these findings, loss of DUSP6 in DLD1 resulted in smaller tumour formation and reduced Ki67 and cleaved Notch1 immunostaining compared to control cells (Fig. 3d–f). Together, these results demonstrate that DUSP6 promotes CRC cell growth both in vitro and in vivo, possibly through Notch1.

https://doi.org/10.1038/s41467-024-54383-y

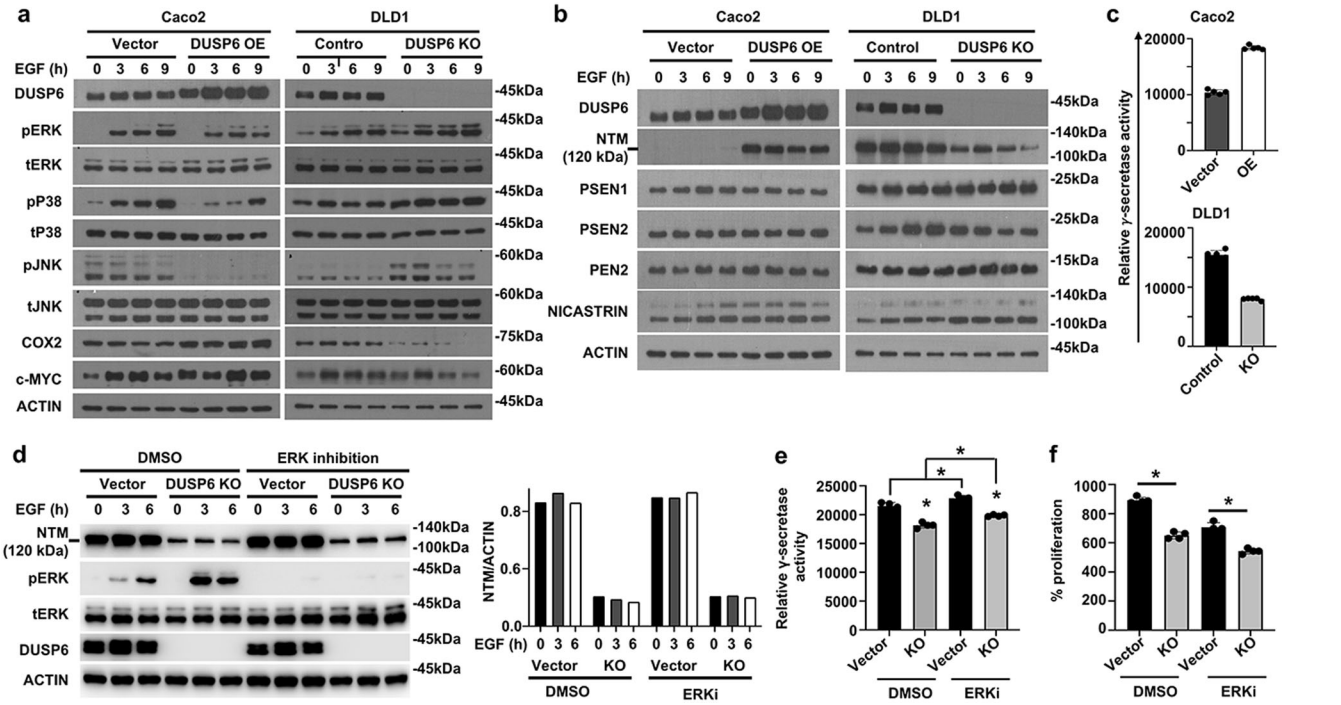

Fig. 2 | DUSP6 negatively regulates the activation of MAPKs and positively regulates the level of Notch1 NTM. a Western blot analysis showing changes in the levels of phosphorylated MAPKs (ERK1/2, P38, JNK) and the expression of target genes upon treatment with 100 ng/mL EGF in Caco2 cells overexpressing DUSP6 (DUSP6 OE) and DLD1 cells with DUSP6 knockout (DUSP6 KO) compared to the respective ppy-vector and sg-vector control cells. **b** Western blots showing the changes in the levels of NTM and components of γ-secretase after treatment with 100 ng/mL EGF. (Data shown in (**a**) and (**b**) is representative of three independent experiments). **c** Assessment of γ-secretase activity in Caco2 and DLD1 cells after treatment with 100 ng/mL EGF for 3 h. ($n = 5$ wells, representative of three independent experiments). **d**–**f** Effects of ERK inhibition on DLD1 DUSP6 KO cells. **d** Western blot analysis showing changes in the levels of NTM and ERK1/2 phosphorylation in DLD1 KO cells with or without ERK inhibition. The blots were analysed by densitometric analysis before the level of NTM relative to ACTIN is calculated and presented in the bar chart. The data shown is representative of two independent experiments. **e** Assessment of γ-secretase activity and (**f**) cell proliferation in vector and DUSP6 KO DLD1 cells with or without ERK inhibition ($n = 4$ biologically independent samples). * denotes $P < 0.05$ (two-tailed, nonparametric, Mann−Whitney test). Error bars = mean ± standard deviations. "OE" and "KO" denote overexpression and knockout, respectively. NTM cleaved Notch1 transmembrane/intracellular domain. Source data are provided as a Source Data file.

To verify the function of DUSP6 in CRC development, we generated a DUSP6-inducible Caco2 cell line using the Tet-on inducible system, whereby DUSP6 expression occurred solely upon doxycycline (Dox) treatment (Supplementary Fig. S6A). Consequently, increased proliferation was observed in DUSP6-inducible OE cells on Day 3 after Dox treatment compared to control or non-treated cells (Supplementary Fig. S6b). Results from western blot analysis demonstrated that the levels of NTM, COX2, and c-MYC were only increased when DUSP6-inducible OE cells were treated with Dox compared to control cells (Supplementary Fig. S6c). Consistently, DUSP6-inducible OE cells formed larger tumours in NSG mice with Dox treatment, compared to those formed by vector cells or DUSP6-inducible OE cells without Dox treatment (Fig. 4a). Immunohistochemical staining of the tumour tissues showed increased DUSP6 and cleaved Notch1 levels only in DUSP6-inducible OE tumours from mice with Dox treatment, but not those from mice treated with saline, compared to tumours formed by vector cells (Fig. 4b, c). Together, these results conformed the tumour-promoting function of DUSP6 in CRC, which was associated with increased NTM.

Loss of DUSP6 in mice results in reduced colonic tumour development

The azoxymethane (AOM)/dextran sodium sulfate (DSS) animal model recapitulates the development of human CRC and highly resembles that of colitis/inflammation-associated CRC[28]. We applied this model to both DUSP6 wildtype (WT) and knockout (KO) mice to assess the role of DUSP6 in CRC tumorigenesis. It was observed that WT mice developed an average of nine colonic tumours with a size of approximately 23 mm^3 (macroscopic measurements) at 16 weeks post-AOM injection (Fig. 4d). In contrast, DUSP6 KO mice developed an average of three colonic tumours of ~10 mm^3 in size. Tumours developed in DUSP6 KO mice were less proliferative as indicated by 43% reduction in Ki67 staining in colonic tumour tissues (Fig. 4e). In addition, there was significantly less cleaved Notch1 staining in tumours from DUSP6 KO mice (Fig. 4f). Together, these results indicate that DUSP6 has pro-tumourigenic function in vivo, which may have resulted from the regulation of Notch1.

DUSP6 inhibits ubiquitin-mediated proteasomal degradation of NICD

The cleaved Notch1 intracellular region acts as a transcriptional activator for the activation of various genes involved in tumour development[29]. Overall cleaved Notch1 intracellular region activity can be regulated via phosphorylation to mark it for ubiquitin-mediated proteasomal degradation[18,30]. Several kinases such as Cdk8, homeodomain-interacting protein kinase 2 (HIPK2), and dual-specificity tyrosine-regulated kinase 2 (DYRK2) were shown to phosphorylate Notch1 for this purpose. However, there is no report of any negative regulators that could dephosphorylate cleaved the Notch1 intracellular region to preserve its cellular activity/abundance. The association between DUSP6 and the level of NTM suggests the possible regulation of NTM by DUSP6. To test this, we examined the interaction between DUSP6 and NTM. Results from the co-immunoprecipitation assay showed that endogenous NTM could bind to Flag-tagged DUSP6 in DLD1 cells (Fig. 5a). Similarly, when HA-tagged NTM was overexpressed in DLD1 cells, and immunoprecipitated with anti-HA beads,

https://doi.org/10.1038/s41467-024-54383-y

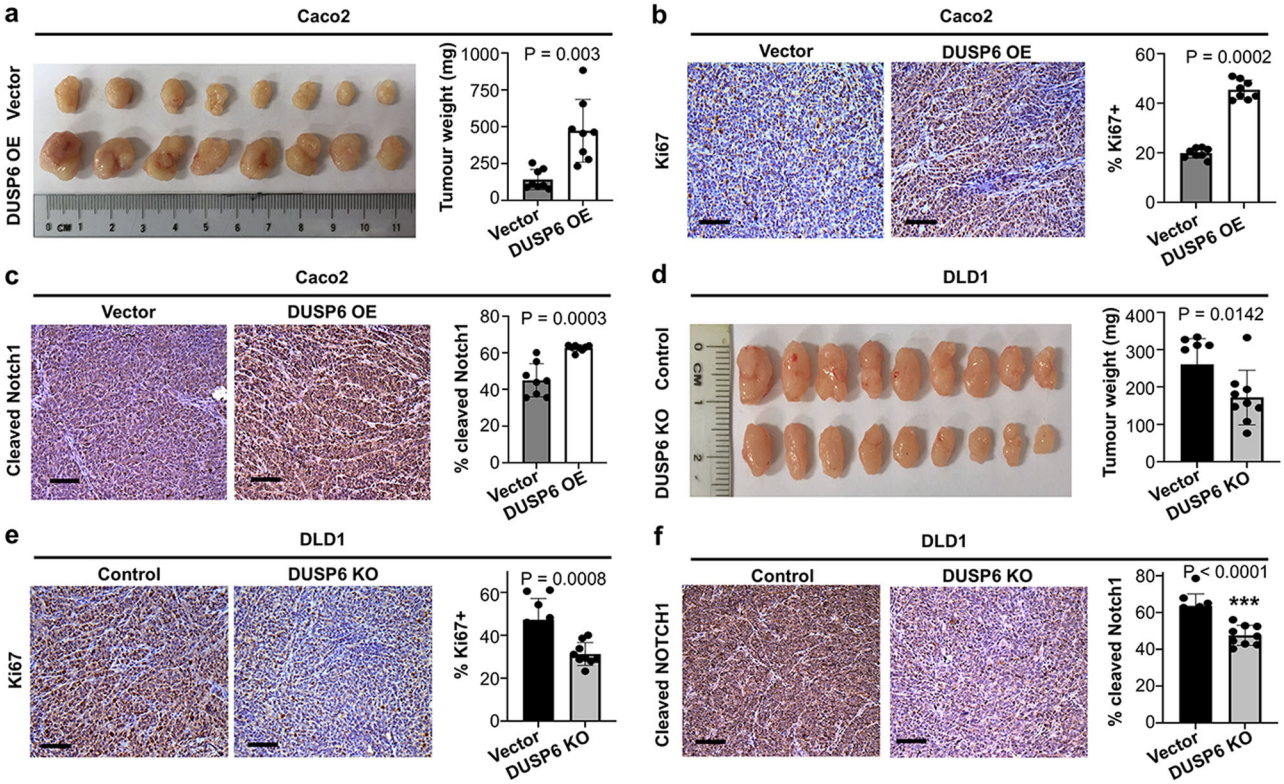

Fig. 3 | DUSP6 expression is positively associated with CRC cell growth in vivo. **a** Representative photographs of Caco2 xenograft tumours and bar chart showing the weight of Caco2 xenograft tumours with or without DUSP6 overexpression ($n = 8$ biologically independent samples). **b**, **c** Representative micrographs and bar charts showing the level of Ki67 and cleaved Notch1 staining in Caco2 xenografts, respectively ($n = 8$ biologically independent samples). **d** Representative photographs of DLD1 xenograft tumours and a bar chart show the weight of DLD1 xenograft tumours ($n = 9$ biologically independent samples). **e**, **f** Representative micrographs and bar charts showing level of Ki67 and cleaved Notch1 staining in DLD1 xenografts respectively ($n = 9$ biologically independent samples). Scale bar = 100 μm. Statistical analysis = two-tailed, nonparametric Mann–Whitney test. Error bars = mean ± standard deviations. "OE" and "KO" denote overexpression and knockout, respectively. The data shown is representative of two independent experiments. Source data are provided as a Source Data file.

endogenous DUSP6 was subsequently detected in the immunoprecipitate of HA-NTM (Fig. 5b). These results confirmed that DUSP6 binds to NTM. Next, we performed an in vitro dephosphorylation assay to test if DUSP6 could dephosphorylate NTM, which was purified from DLD1 cells. The results showed that the amount of total phosphotyrosine on NTM was reduced by ~55% when incubated with DUSP6 (Fig. 5c). Similarly, DUSP6 was able to dephosphorylate endogenous NTM immunoprecipitated from Caco2 cells (Supplementary Fig. S7). These results demonstrated that DUSP6 is able to dephosphorylate NTM directly.

Next, we performed a sequential dephosphorylation and ubiquitination experiment to test if the dephosphorylation of NTM by DUSP6 could lead to reduced ubiquitination. NTM was purified from DLD1 by immunoprecipitation, after which it was incubated with DUSP6 for dephosphorylation. The resultant NTM was then used as input for in vitro ubiquitination assay. Consistent with previous data (Fig. 5c), a reduction in total phospho-tyrosine was detected after NTM was incubated with DUSP6 (Fig. 5d, top bar chart). Importantly, the amount of ubiquitination on the dephosphorylated NTM was reduced by ~38% compared to the control (Fig. 5d, bottom bar chart). These results demonstrated that dephosphorylation of NTM by DUSP6 could lead to reduced ubiquitination of NTM.

Ubiquitination of NTM is followed by proteasome degradation. To address if the reduced ubiquitination of NTM triggered by DUSP6 could lead to changes in proteasomal-mediated degradation, we treated DUSP6 KO and control DLD1 cells with MG132, a potent proteasome inhibitor, followed by examination of the levels of NTM. It was found that DUSP6 KO cells had more than 2-fold lower NTM than the vector control cells (Fig. 5e). When proteasome was inhibited by treatment with MG132, NTM level was increased by 2.8- and 2.6-folds at 10 and 15 hours in control cells. In contrast, the level of NTM was increased by 5.8- and 5.0-folds in the KO cells treated with MG132 compared to KO cells without MG132 treatment. As such, the difference in NTM levels between DUSP6 KO and vector control cells after treatment with MG132 was reduced to only 1.3-fold. We also confirmed the negative association between DUSP6 and ubiquitinated NTM levels in Caco2 DUSP6 OE and DLD1 DUSP6 KO cells. In Caco2 DUSP6 OE cells where the NTM level was higher than the vector control cells, the proportion of ubiquitinated NTM (relative to total NTM) was ~3-fold lower than the control cells (Fig. 5f). Conversely, the ratio of ubiquitinated NTM was 1.4-fold higher in DLD1 DUSP6 KO cells compared to that in control cells. Together, these results demonstrate that DUSP6 inhibits NTM ubiquitination to enhance its stability.

DUSP6-mediated CRC cell proliferation is Notch1 dependent

To verify if DUSP6 regulates CRC cell proliferation through Notch1, we knocked out *NOTCH1* in Caco2 DUSP6 OE cells, followed by an examination of cell proliferation. Consistent with previous results (Fig. 1), DUSP6 OE cells had increased proliferation compared to vector control cells (Fig. 6a, bar 3 vs bar 1). However, when the *NOTCH1* gene was deleted from vector control cells, cell proliferation was significantly reduced on days 2 and 3 compared to vector control cells (Fig. 6a, bar 2 vs bar 1). Importantly, when the *NOTCH1* gene was deleted from Caco2 DUSP6 OE cells, cell proliferation became comparable to that of vector control cells (Fig. 6a, bar 4 vs bar 1). Western blot analysis showed that there was no NTM after *NOTCH1* gene was

https://doi.org/10.1038/s41467-024-54383-y

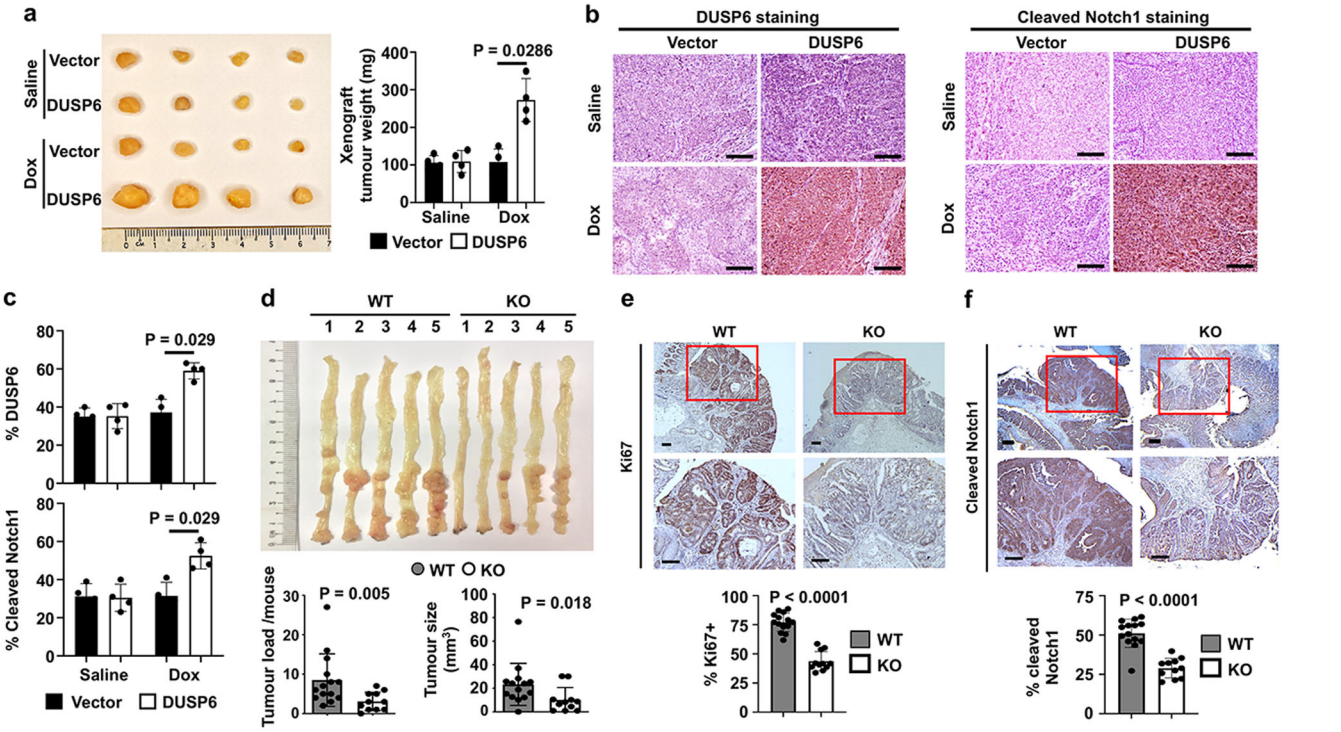

Fig. 4 | Induced expression of DUSP6 promotes CRC growth and loss of DUSP6 in mice resulted in reduced colonic tumour development. a Caco2 cells transfected with Tet-on vector and full-length DUSP6 cDNA were subcutaneously injected into NSGS mice (5×10^6 cells per mice). Mice (8–10 weeks old) were treated with doxycycline (Dox) (1 mg/kg) or saline twice a week for 4 weeks before assessment of tumour growth. The bar chart shows the weight of Caco2 xenograft tumours with or without Dox treatment ($n = 4$ biologically independent samples). **b** Representative micrographs of immunohistochemical staining and (**c**) bar charts showing the level of DUSP6 and cleaved Notch1 staining in the xenograft tumour tissues ($n = 4$ biologically independent samples). **d** Representative photograph of colonic tumours found in wildtype (WT) and DUSP6 knockout (KO) mice given AOM/DSS for induced tumour development. Bar charts show the total number of colonic tumours and the average size of tumour found in each mouse (WT $n = 14$, KO $n = 11$). **e** Representative micrographs showing Ki67 staining in the tumours from WT and DUSP6 KO mice (8–10 weeks old). Boxed areas are shown magnified in the bottom panels. The percentage of Ki67 positive cells per tumour is shown in the bar chart (WT $n = 14$, KO $n = 11$). **f** Representative micrographs showing cleaved Notch1 staining in the tumours from WT and DUSP6 KO mice (8–10 weeks old). Boxed areas are shown magnified in the bottom panels. The percentage of cleaved Notch1 positive cells per tumour is shown in the bar chart (WT $n = 14$, KO $n = 11$). Scale bar = 100 μm. Statistical analysis = two-tailed, nonparametric Mann–Whitney test. Error bars = mean ± standard deviations. Source data are provided as a Source Data file.

deleted (Fig. 6b). In addition, COX2 levels became comparable between vector control and DUSP6 OE/NOTCH1 KO cells, and c-MYC was reduced in Caco2 DUSP6 OE/NOTCH1 KO compared to Caco2 DUSP6 OE/PX458 vector control (Fig. 6b). These results suggest that DUSP6 regulates CRC cell proliferation through Notch1.

Dephosphorylation of phospho-Y2116 of Notch1 by DUSP6 is critical for its regulation of CRC cell proliferation

To further confirm that DUSP6 could dephosphorylate phosphotyrosine residue on NTM and regulate the level of Notch1 activity, mass spectrometry analysis was employed to screen for phospho-sites on NTM that may be targeted by DUSP6. A total of 17 phospho-serine, 3 phospho-threonine and 2 phospho-tyrosine were detected in the NTM purified from Caco2 vector cells (Table 1). Of which, phospho-Y2116 (p-Y2116) was the only tyrosine residue that had lost its phosphorylation when DUSP6 was overexpressed. In addition, two serine residues, S1951 and S2205, had also lost their phosphorylation in DUSP6 OE cells. Next, to test the importance of p-Y2116, p-S1951 and p-S2205 in Notch1 signalling, we generated Notch1 mutants in which the tyrosine residue at position 2116 (Y2116), the serine residue at position 1951, or the serine residue at position 2205 were changed to alanine (Y2116A, S1951A and S2205A) respectively. Using the CSL (CBF1/RBP-Jκ) reporter and the Notch1 pathway reporter assay, we found that overexpression of DUSP6 resulted in increased Notch1-mediated transcriptional activity (Fig. 6c). Interestingly, only in cells with NICD Y2116A, but not in those with NICD S1951A or S2205A, the transcriptional activity was increased compared to cells with wildtype NTM without DUSP6 overexpression (NTM FL + vector vs NTM Y2116A + vector; $P = 0.0007$). This observation suggests that among the three mutations, only the Y2116A mutation rendered NTM with the capacity to escape ubiquitination and, subsequently, proteasomal degradation. To further verify the importance of Y2116 in DUSP6-regulated Notch1 signalling, we transfected NTM WT or NTM Y2116A into DUSP6 KO DLD1 cells, followed by measurement of cell proliferation. The results demonstrated that both NTM WT and NTM Y2116A were able to rescue the reduced proliferation of DUSP6 KO cells (Fig. 6d). Together, these results suggest that Y2116 is the phospho-site that is targeted by DUSP6 to control Notch1 activity.

High DUSP6 protein expression is associated with high NICD levels and worse overall survival in CRC patients

To further verify the regulation of NTM by DUSP6, we examined the levels of DUSP6, full-length Notch1 and NTM in 10 human CRC cell lines, including DLD1, Caco2, OUMS23, RCM1, SW480, HCT116, HCC56, Colo205 and LoVo, by western blot. Nonparametric Spearmen correlation analysis of the results showed that the level of DUSP6 is positively associated with the level of NTM, but not the full-length Notch1 (Supplementary Fig. S8a).

Next, DUSP6 protein expression in primary tumours and adjacent normal tissues from 81 CRC patients were analysed by immunostaining. Results revealed higher DUSP6 expression in adenocarcinoma cells in tumour tissues compared to the surrounding tumour stroma

Table 1 | Mass spectrometry screening for Notch1 phosphorylated amino acid residues

Caco2 vector control		Caco2 DUSP6 overexpression	
Amino acid	Site	Amino acid	Site
S	1801	S	1801
T	1861	T	1861
S	1951	Not detected	
T	1897	T	1897
S	1900	S	1900
S	1970	S	1970
Y	2116	Not detected	
S	2121	S	2121
T	2132	T	2132
S	2136	S	2136
S	2141	S	2141
Y	2145	Y	2145
S	2170	S	2170
S	2194	S	2194
S	2198	S	2198
S	2202	S	2202
S	2205	Not detected	
S	2215	S	2215
S	2221	S	2221
S	2290	S	2290
S	2303	S	2303
S	2516	S	2516

(Fig. 7a). Whereas in normal adjacent tissues, DUSP6 was expressed in crypt epithelial cells as well as cells in the luminal propria, sub-mucosa and muscularis. Overall, increased DUSP6 expression was identified in tumours compared to matched normal adjacent tissues. On the other hand, there were no significant differences in DUSP6 expression in tumours from patients at various stages of disease (Supplementary Fig. S8b). When patients were grouped based on tumour DUSP6 expression level for Kaplan–Meier analysis and the log-rank test, we found that high DUSP6 in tumours is associated with overall poorer survival compared to patients with low tumour DUSP6 expression (median overall survival, 60.5 vs. 67.8 months respectively, $P = 0.029$) (Fig. 7b). Survival rate was approximately 20% lower after ~60 months post-first diagnosis of the disease in patients with high DUSP6 expression. Furthermore, compared to normal adjacent tissues, increased cleaved Notch1 levels were detected in tumour tissues (Fig. 7c), which was positively correlated with the level of DUSP6 (Fig. 7d). These results suggest that DUSP6 influence tumour development and in turn the clinical outcome of CRC through regulation of NTM.

Discussion

Notch1 signalling is important for various cellular activities, including cell growth, migration, cell cycle arrest and cell death. Dysregulation of Notch1 signalling can promote the development of various types of cancer, including T-cell acute lymphoblastic leukaemia, breast cancer, lung cancer and colorectal cancer[18,31]. Notch1 activity is regulated by posttranscriptional modifications, including phosphorylation and ubiquitination of its intracellular domain which can subsequently translocate to the nucleus to regulate target gene expression upon release. Several protein kinases, including Cdk8, HIPK2 and DYRK2, have been shown to phosphorylate serine/threonine residues in the PEST domain of Notch1[30,32,33]. These phosphorylation events could lead to FBXW7 ubiquitin E3 ligase-mediated degradation, thereby inhibiting the transcriptional activity of Notch1 target genes. However, it is unclear if such phosphorylation could be reversed by specific phosphatases. Here we demonstrated that DUSP6 is a Notch1 phosphatase that dephosphorylates p-Y2116, thereby reducing NTM ubiquitination and proteasome degradation. This leads to enhanced stability and transcriptional activity of Notch1 in CRC cells to promote growth and CRC development. As such, DUSP6 KO mice developed less tumours with smaller sizes compared to WT mice, associated with reduced NTM in response to DSS/AOM treatment (Fig. 4d–f). Markedly, in CRC patients, the expression of DUSP6 protein was positively correlated with Notch1 levels, and patients with higher DUSP6 expression in tumours had reduced survival compared to those with lower DUSP6 (Fig. 7). Together, these findings demonstrated that DUSP6 is a Notch1 phosphatase which promotes CRC development through regulation of NTM stability and transcriptional activity.

DUSP6 was previously identified as a MAPK phosphatase that preferentially dephosphorylates ERK1/2 to p38 and JNK[34]. While others have shown a possible association of DUSP6 expression with the pathogenesis of various cancers, the role of DUSP6 in colorectal cancer (CRC) has not been clearly defined. In this study, we showed that tumoral DUSP6 protein expression is significantly increased in tumours from CRC patients compared to paired normal adjacent tissues (Fig. 7). Unlike the previous study that showed reduced tissue DUSP6 mRNA transcripts[35] in advanced CRC tumours, we measured DUSP6 protein in the tumour and normal epithelial tissues via IHC staining to better evaluate DUSP6 expression independent of other host cells such as immune cells, connective tissues and tumour stroma in patients' specimens. It is also important to note that DUSP6 transcripts are prone to post-transcriptional modification by MEK/ERK signalling and is enhanced by hypoxia, a condition that is commonly found in solid tumours[36]. Moreover, mRNA transcripts level may not necessarily translate to protein level without extensive mathematical corrections, and the ratio of mRNA and proteins are not constant for most genes[37]. Measurement of DUSP6 protein level in the tumour and adjacent normal epithelial cells by immunostaining provides a more reliable result for the examination of the possible influence of DUSP6 on patient outcome (there was no survival data from Beaudry, K *et al*). Nevertheless, further analysis identified a negative association between tumoral DUSP6 protein level and CRC clinical outcome. Based on Kaplan–Meier survival analysis, high DUSP6 protein expression in the tumours was associated with worse survival outcomes with ~20% lower survival rate (Fig. 7b). Thus, our study shows the association of tumoural DUSP6 protein levels with cleaved Notch1 and patient survival in CRC. DUSP6 was also reported to be negatively associated with survival in another gastrointestinal cancer. Wu et al. reported that high DUSP6 was found in gastric tumours and was associated with poorer overall and progression-free survival in gastric cancer patients[38]. In addition to mere association, our study provided evidence showing how DUSP6 controls the growth of CRC cells through Notch1.

Of the three MAPKs, ERK1/2 is a critical regulator during tumour cell development. High ERK1/2 activation was found in cancer cells with a high proliferation rate and contributed to metastasis and cell mobility[39]. However, other than the level of pERK1/2, the duration and location of activated ERK/1/2 may have an impact on cellular functions. For example, sustained ERK activation could result in cell cycle arrest due to disruption of overall interaction between DUSP6 and ERK1/2[40]. On the other hand, p38 and JNK, known to be involved in stress responses, could also influence cell survival and apoptosis[6]. Interestingly, while DUSP6 negatively regulates all three MAPKs, it did not exert negative regulatory function against proliferation-associated genes, including COX2 and c-MYC, which are targets of MAPKs, particularly ERK1/2[41] (i.e. increased DUSP6 which led to reduced pERK1/2 did not result in reduced COX2 and c-MYC) (Fig. 2a, b). This thereby implied that DUSP6 regulates CRC development through an alternative mechanism, rather than MAPKs. Therefore, it is plausible that

https://doi.org/10.1038/s41467-024-54383-y

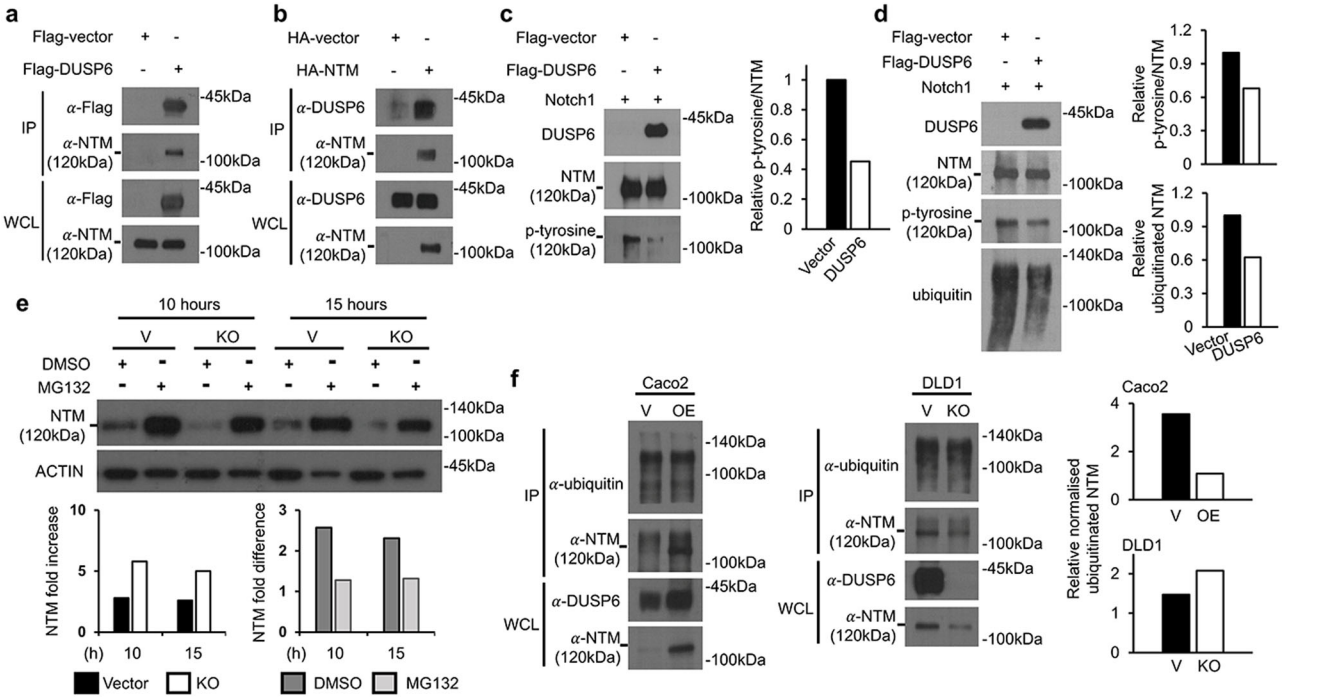

Fig. 5 | DUSP6 binds and dephosphorylates cleaved Notch1, thereby regulating its ubiquitination and proteasomal degradation. a Western blots showing endogenous cleaved Notch1 immunoprecipitated with Flag-DUSP6 in DLD1 cells. **b** Western blots showing endogenous DUSP6 immunoprecipitated with HA-NTM in DLD1 cells. **c** Western blots show dephosphorylation of NTM purified from DLD1 cells using immunoprecipitation. The blots were analysed by densitometric analysis before the level of total p-tyrosine on NTM is calculated and presented in the bar chart. **d** Western blots show results from sequential dephosphorylation of NTM and ubiquitination of the dephosphorylated NTM in vitro. NTM was purified from DLD1 cells by immunoprecipitation. Blots were analysed by densitometric analysis before the level of total p-tyrosine on NTM and total ubiquitinated NTM are calculated and presented in the bar charts. **e** Western blots show the changes in NTM level in DLD1 DUSP6 KO and sg-vector control cells after treatment with MG132 for 10 and 15 h to inhibit proteasomal degradation. Blots were analysed by densitometric analysis before the changes in NTM level are calculated and presented in the bar charts. **f** Western blots show the level of endogenous ubiquitinated NTM from the respective Caco2 and DLD1 cells. Blots were analysed by densitometric analysis before the ratio of ubiquitinated NTM are calculated and shown in the bar charts. Data shown in (**a**–**c**), (**e**, **f**) are representative of three independent experiments, (**d**) is representative of two independent experiments. Source data are provided as a Source Data file.

DUSP6 could positively regulate cellular proliferation and migration of CRC cells through Notch1.

The release of cleaved Notch1 following ligand binding of Notch receptor requires the cleavage by γ-secretase, which is a multimeric complex made up of PSEN1 or PSEN2, NCSTN, anterior pharynx defective 1 (APH-1), and presenilin enhancer 2 (PEN2). However, the absolute amount of each γ-secretase component may not be the sole factor that controls its catalytic activity. It has been shown that NCSTN and PSEN1 can be phosphorylated by ERK1/2 to regulate γ-secretase activity for cleavage of amyloid protein precursor[42], suggesting that post-translational regulation of γ-secretase components could regulate γ-secretase activity. Interestingly, it has been shown that phosphorylation of PSEN1 on serine 367 did not affect γ-secretase activity toward β-amyloid precursor protein (APP) but reduced its activity toward Notch[43,44]. On the other hand, phosphorylation of NCSTN by ERK1/2 resulted in reduced γ-secretase activity without changing its protein expression[45]. In this study, we did not observe changes in the expression level of the four components of γ-secretase in both DUSP6 OE Caco2 and DUSP6 KO DLD1 cells compared to their respective control (Fig. 2b) but observed increased γ-secretase activity in DUSP6 OE Caco2 cells and conversely decreased γ-secretase activity in DUSP6 KO DLD1 cells (Fig. 2c). The endogenous γ-secretase activity was negatively associated with pERK1/2 level in both types of CRC cells, which is in line with previous findings on the negative regulation of γ-secretase activity by ERK1/2[27,45]. These results suggest that DUSP6 positively regulate γ-secretase activity through a post-translational modification, possibly through ERK1/2. Indeed, when ERK1/2 phosphorylation was inhibited in vector and DUSP6 KO DLD1 cells, γ-secretase activity was increased (Fig. 2e). The detailed mechanisms underlying the regulation of γ-secretase activity by ERK1/2 are unclear. It is likely that the phosphorylation of NCSTN and PSEN1 by ERK1/2 changed their interaction with substrates, thereby influencing the enzymatic activity of γ-secretase and probably also substrate preference, which requires further investigation. However, despite the increase of γ-secretase activity in DLD1 KO cells upon ERK1/2 inhibition, the NTM levels remain unchanged in both vector and KO cells. One possible explanation is that cleaved Notch1 is more potently regulated at the post-translational level, and the ERK1/2-regulated γ-secretase activity is not powerful enough to cause a detectable change in NTM level. Another possibility is that the modification of γ-secretase by ERK1/2 in this case did not increase its substrate affinity toward Notch1 but instead affected its preference toward other substrates, however this requires further investigation.

While the generation of cleaved Notch1 is primarily regulated by γ-secretase, the activity of cleaved Notch1 intracellular region is regulated by post-translation modification processes such as phosphorylation-dependent proteasomal degradation[30]. The majority of the predicted Notch1 phosphorylation sites reported are based on high throughput mass spectrometry analysis[46]. The physiological relevance of these phospho-sites is largely unknown. Studies have shown the importance of FBXW7 ubiquitin E3 ligase recognising phosphorylated Thr-2512 of Notch1 to target the cleaved Notch1 for ubiquitination and subsequent proteasomal degradation[30]. An outstanding question that is underreported pertains to the modulation of Notch1 activities by dephosphorylation and the corresponding biological impact. There is no answer to this question in the current

https://doi.org/10.1038/s41467-024-54383-y

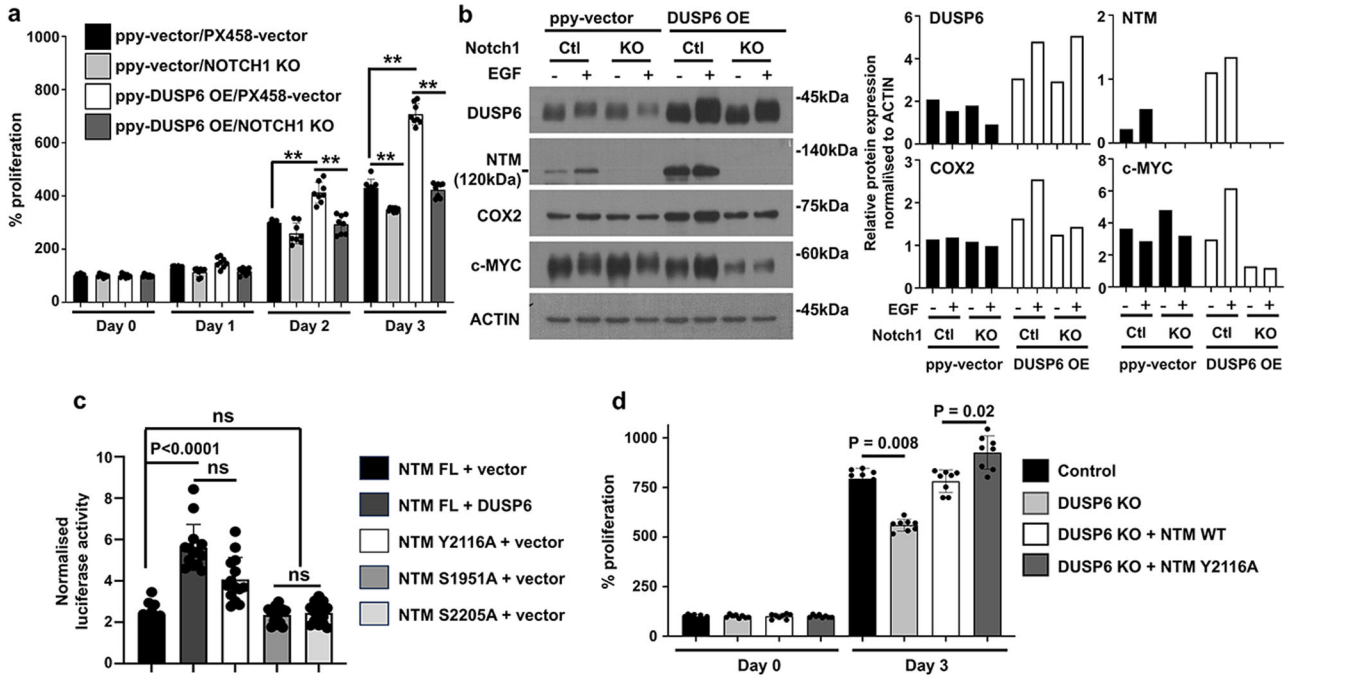

Fig. 6 | Regulation of tumour cell proliferation by DUSP6 is Notch1 dependent. **a** Bar chart shows the effect of DUSP6 expression and loss of NOTCH1 gene on the rate of Caco2 cell growth ($n = 8$ biologically independent samples). **b** Western blot analysis showing changes in protein expression of NTM and target genes after treatment of Caco2 cells with 100 ng/mL EGF for 3 h. Blots were analysed by densitometric analysis before the ratio of each target protein to ACTIN are calculated and shown in the bar charts. "OE", "KO" and "Ctl" denote overexpression, knockout and control, respectively. The data shown is representative of two independent experiments. **c** Bar chart shows the level of cleaved Notch1-mediated Notch1 pathway activity using Notch1 reporter assay ($n = 14$ biologically independent samples). **d** Bar chart shows the growth of DUSP6 control and KO DLD1 cells with or without transfection of NTM WT or NTM Y2116A mutant ($n = 8$ biologically independent samples). ** and "ns" denote $P < 0.01$ and "not significant", respectively (ANOVA Kruskal–Wallis, Dunn's multiple comparisons test). Error bars = mean ± standard deviations. Source data are provided as a Source Data file.

literature. In this study, we demonstrated that DUSP6 interacts with and dephosphorylates NTM, resulting in decreased ubiquitination (Fig. 5a–d), and consequently increased NTM levels. The total amount of endogenous ubiquitinated NTM was negatively correlated with DUSP6 expression (Fig. 5f). Furthermore, treatment of DUSP6 KO DLD1 cells with proteasome inhibitor MG132 largely restored the level of NTM (Fig. 5e). Together, these results confirmed that DUSP6 regulates NTM mainly through a proteasomal-dependent mechanism.

As mentioned earlier, multiple phosphorylation sites were predicted on Notch1. However, antibodies for specific phospho-Notch1 are not available commercially. Therefore, mass spectrometry analysis was carried out to identify the potential phosphorylation sites that are targeted by DUSP6. This led to the identification of phospho-Y2116 residue in this study. Overexpression of DUSP6 resulted in dephosphorylation at Y2116, reduced ubiquitination and increased NTM level, suggesting that phosphorylation of Y2116 also leads to ubiquitination and proteasomal degradation of NTM. However, the identity of Y2116 phosphorylating kinases and the corresponding ubiquitin ligases warrants further investigation. Functionally, we confirmed that this residue is important for Notch1 activity, whereby mutation resulting in Y2116A leads to increased Notch1 activity since this site is no longer targeted for phosphorylation and ubiquitination. Indeed, this mutation resulted in a similar effect as DUSP6 overexpression on the transcriptional activity of NTM (Fig. 6c). Together, our study showed that DUSP6 expression induced CRC tumour cell growth by dephosphorylating phospho-Y2116, thereby positively regulating NTM level. This mechanism could potentially be targeted in patients for CRC therapy.

DUSP6 has been shown to play an important role in the regulation of hepatic glucose metabolism. Increased expression of *Dusp6* was detected in the insulin-resistant liver from diet-induced and genetically obese mice (e.g. *ob/ob* and *db/db* mice) compared to their respective control[47,48]. Overexpression of *Dusp6* in the liver of lean mice promoted hepatic gluconeogenesis and insulin resistance, whereas liver-specific knockdown of this molecule led to reduced hepatic gluconeogenesis, improved glucose tolerance and insulin sensitivity[48]. It was further found that DUSP6 promotes hepatic gluconeogenesis through activation and promoting nuclear translocation of Forkhead box O1 (FOXO1) protein to induce the expression of gluconeogenic genes such as *Glucose-6-phosphatase (G6pase)*. Interestingly, Notch1 also plays a crucial role in the regulation of hepatic glucose production, which is dependent on FOXO1. This mechanism relies on the association of Notch1 with FOXO1 to induce the expression of *G6pase*, thereby promoting hepatic gluconeogenesis[49]. Together, these studies suggest the possible link between DUSP6 and Notch1 in the regulation of hepatic gluconeogenesis. It is possible that DUSP6 dephosphorylates and increases the stability of Notch1, leading to increased activation of FOXO1 and expression of hepatic gluconeogenic genes such as G6pase. Further investigation is warranted to confirm this possible mechanism underlying the function of DUSP6 in hepatic gluconeogenesis and metabolic disorders.

In summary, we showed that DUSP6 is a Notch1 phosphatase which regulates Notch1 intracellular protein level through phosphorylation-dependent, ubiquitin-mediated proteasomal degradation. Phospho-Y2116 is the main target of DUSP6 for this purpose. Through dephosphorylation of phospho-Y2116, DUSP6 reduces NTM ubiquitination and proteasomal degradation. Increased expression of DUSP6, therefore, increases NTM level and, in turn, transcriptional activity to promote CRC development. Our discoveries, therefore, shed light on the regulation and function of Notch1 in cancer and provide a new avenue for targeting Notch1 signalling to develop therapy for human diseases.

https://doi.org/10.1038/s41467-024-54383-y

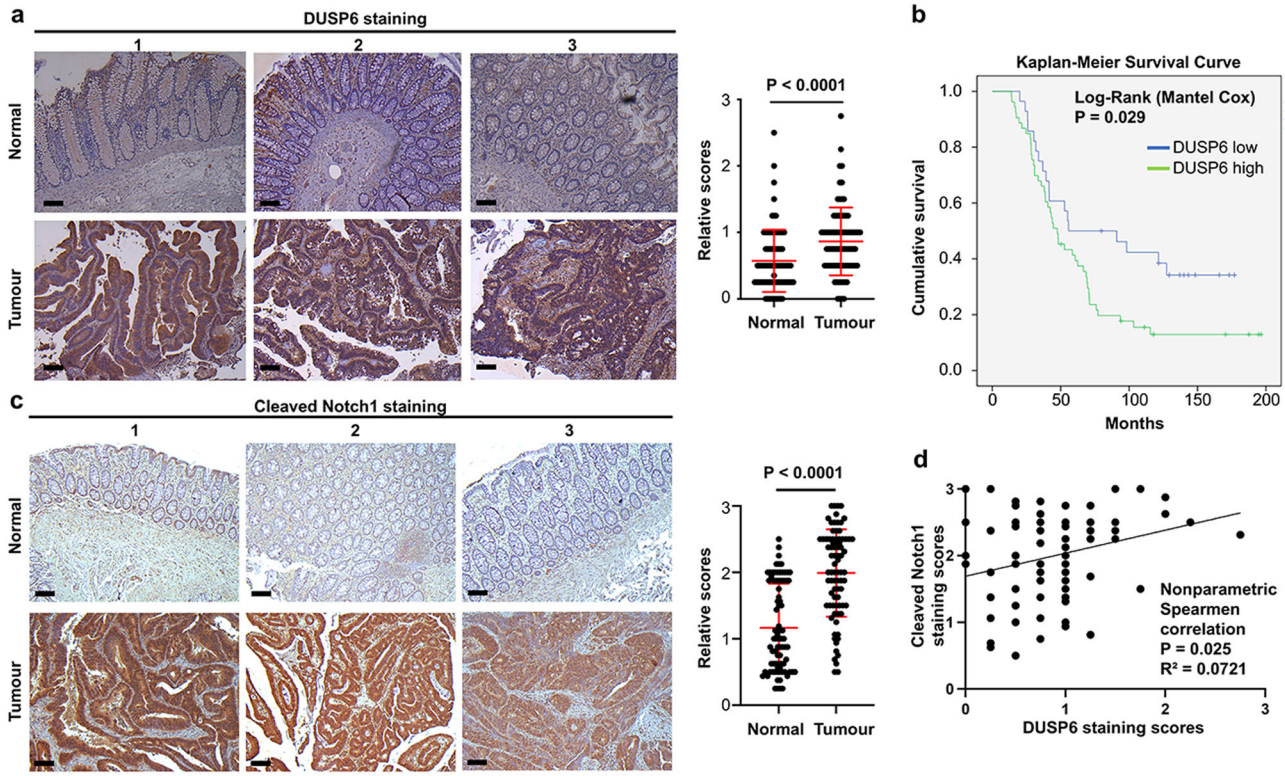

Fig. 7 | High DUSP6 expression in CRC tumours is associated with higher cleaved Notch1 levels and worse overall survival in CRC patients. **a** Representative micrographs showing DUSP6 staining in tumours and normal adjacent tissues from CRC patients. Scale bar = 100 μM. Dot-plot shows the comparisons of the level of DUSP6 staining in normal and tumour tissues, Statistical test = two-tailed, nonparametric, Mann–Whitney test. Error bars = mean ± standard deviations. **b** Kaplan–Meier survival curve and log-rank (Mantel–Cox) test showing overall survival of CRC patients stratified by high or low DUSP6 expression in tumours cells. **c** Representative micrographs showing cleaved Notch1 staining in tumours and normal adjacent tissues from CRC patients. Scale bar = 100 μM. Dot-plot shows the comparisons of the level of cleaved Notch1 staining in normal and tumour tissues. Statistical test = two-tailed, nonparametric, Mann–Whitney test. Error bars = mean ± standard deviations. **d** Dot-plot shows the correlation between the levels of DUSP6 and cleaved Notch1 in tumours from patients. Normal samples $n = 81$; tumour samples $n = 81$. Source data are provided as a Source Data file.

Methods

Animal studies

All animal studies conformed to ethical compliance were approved by NUS Institutional Animal Care and Use Committee (IACUC). DUSP6 knockout (KO) male mice (Jackson Laboratory (Bar Harbor, USA) were backcrossed with local C57BL/6J mice for ten generations, and the subsequent offspring of DUSP6 wildtype (WT) and DUSP6 KO mice were maintained in-house. NSGS mice were obtained from Jackson Laboratory and were inbred for all xenograft experiments in this study. The DUSP6 WT and KO mice used in this study are 8–10 weeks old, whereas NSGS mice are 6–8 weeks old.

Colonic tumours were induced in mice by treatment with azoxymethane (AOM) and dextran sodium sulfate (DSS)[50]. Briefly, male mice were given a single administration of 10 mg/kg of AOM in sterile saline via intraperitoneal injection before initiation of three cycles of 1% DSS ad libitum for 5 days with 2 weeks rest starting from Day 7 post AOM injection. Mice were sacrificed to determine the colonic tumour load at Week 16 post-AOM injection. For establishment of colorectal cancer cell line xenograft model, 5×10^6 Caco2 cells stably overexpressing DUSP6 (or ppy-vector control); or DUSP6 KO (or sgRNA-vector control) DLD1 cells were subcutaneously injected into the flanks of either male or female NSGS mice. Caco2 DUSP6 OE or DLD1 DUSP6 KO cells were injected in the left flank, whereas the respective control cells were injected in the right flank of each mouse. Tumour xenografts were allowed to develop over 3 weeks before harvest. All the xenograft tumours are less than the maximal combined tumour size of 1.5 cm as permitted by NUS IACUC.

Clinical specimens and survival analysis

A total of 81 CRC patients were included in this study, and the clinical features are summarised in Supplementary Table 1. Access to archival tissue sections and patient demographics was approved by the National Health Group, Domain Specific Review Board (NHG DSRB). Informed consent was obtained for these specimens to be used for research purposes. The survival curve was calculated by using the Kaplan–Meier method, whereas the significance was determined by the log-rank test. Patients were stratified based on DUSP6 expression level in the tumours as assessed by immunohistochemical staining (see Immunohistochemistry section in Supplementary Material and Methods). Median expression value was used as the cut-off for selection of DUSP6 high (53 out of 81) or low group (28 out of 81).

Western blot analysis

Western blot analysis was performed as described previously[50]. Briefly, cells were harvested at respective timepoints in lysis buffer (1 M Tris-Cl, 5 M NaCl, 10% NP40) containing 1x phosphatase inhibitor (Roche, Switzerland) and 1x protease inhibitor (Roche) before quantification using Bio-Rad Bradford reagent. Protein lysates were resolved in Tris/Glycine gel (10 or 12% acrylamide, 1.5 M Tris (pH8.8), 10% SDS, 10% APS, TEMED) before transferred to PVDF membrane for detection of proteins (see Supplementary Table 2. 'Antibodies and immunoprecipitation beads used in this study' for information of antibodies used). ImageJ software was used for western blot densitometry analysis where required[25]. To note, the Notch1 antibody

from Cell Signaling (D1E11/#3608) can detect both the full-length Notch1 protein (~300 kDa) and the cleaved Notch1 intracellular domain together with a short extracellular juxtamembrane peptide and a transmembrane sequence (120 kDa, referred to as 'NTM' in this study). This antibody was used for all Western blot analyses to detect the cleaved Notch1 intracellular domain region. For immunostaining to detect cleaved Notch1 intracellular region, the Abcam antibody #ab52301 was used. This antibody detects the fragment of activated cleaved Notch1 resulting from cleavage adjacent to Val1744 of Notch1.

In vitro dephosphorylation and ubiquitination

For the dephosphorylation assay, 0.9×10^6 293T cells in a six-well plate were transfected with Flag-tagged DUSP6 or HA-tagged NICD plasmid using TransIT®-293 Transfection Reagent (Mirus Bio LLC, USA) to overexpress the respective proteins overnight. Cells were lysed in NP40 lysis buffer before purification of target proteins by immunoprecipitation. To note, a phosphatase inhibitor was not added to the lysis buffer for cells transfected with Flag-DUSP6 to preserve the phosphatase activity. Proteins were purified by immunoprecipitation using the respective Tag beads for 2 h at 4 °C. Purified proteins bound to the beads were washed 3x with sterile PBS and used for dephosphorylation assay. For purification of endogenous NICD protein, 1.8×10^6 DLD1 cells were treated with 10 μM proteasome Inhibitor MG132 for 16 h, after which the proteins were lysed with NP40 lysis buffer and subsequently purified by immunoprecipitation using 1/50 dilution of anti-Notch1 antibody and 1/25 dilution of Protein A/G magnetic beads (Sigma) for 2 h at 4 °C. All the protein-bound beads were divided into tubes equally and used in the respective dephosphorylation reactions. About 300 μL of dephosphorylation buffer containing 50 mM HEPES, 100 mM NaCl, 1 mM MnCl2, 2 mM DTT, 0.1 mM EGTA and 0.025 % Tween 20 was added to the protein-bound beads and incubated at 37 °C for 1.5 h before purification of the beads for Western blot analysis.

In vitro ubiquitination was carried out using the Abcam ubiquitylation assay kit with slight modifications. Equal proportions of input endogenous NTM protein (immunoprecipitated from DLD1 cells using anti-Notch1 antibody and magnetic A/G beads) that were subjected to in vitro dephosphorylation was added to the in vitro ubiquitination reaction (total volume of 50 μL). Each reaction contained 5 nM E1, 100 nM E2, 20 nM FBW7 E3 ligases and 2 mM ATP in 1X ubiquitination buffer (Abcam). The mixture was incubated at 30 °C for 1 h before analysis using Western blot.

Notch1 reporter assay

Activation of the Notch1 pathway was assessed using the Notch1 Pathway Reporter Kit (BPS Bioscience, USA) based on the manufacturer's instructions with modification. Briefly, 293T cells seeded in 96-well plates were transfected with 60 ng of CSL (CBF1/RBP-J κ) luciferase reporter vector plasmid together with either 100 ng of DNA plasmid to overexpress wildtype or mutation NTM with or without ppy-DUSP6 (ppy-vector as control for DUSP6). Transfected cells were left to grow overnight before detection of the luciferase activity using the Dual-Glo® Luciferase Assay System (Promega, USA). To note, three mutant NTM constructs were made by creating point mutation in the wildtype NTM construct at either position 2116 (Y2116A), 1951 (S1951A) or 2205 (S2205A) where the tyrosine or serine residues were mutated to alanine at these positions.

Statistical analysis

All statistical analyses were performed using GraphPad Prism v10.0.3 (217) software (GraphPad; CA, USA). Two-tailed, nonparametric, Mann–Whitney test was used in all comparisons unless otherwise stated. Additional information is available in Supplementary Methods.

Reporting summary

Further information on research design is available in the Nature Portfolio Reporting Summary linked to this article.

Data availability

The raw mass spectrometry spectra and search data were uploaded to the jPost repository with the following accession numbers: JPST002116 (jPOST, https://repository.jpostdb.org/entry/JPST002116) and PXD041338 (ProteomeXchange, https://proteomecentral.proteomexchange.org/cgi/GetDataset?ID=PXD041338). The remaining data were available within the Article, Supplementary Information or Source Data file. Source data are provided with this paper.

References

1. Cancer Genome Atlas N. Comprehensive molecular characterization of human colon and rectal cancer. *Nature* **487**, 330–337 (2012).
2. de la Cruz-Morcillo, M. A. et al. P38MAPK is a major determinant of the balance between apoptosis and autophagy triggered by 5-fluorouracil: implication in resistance. *Oncogene* **31**, 1073–1085 (2012).
3. Karapetis, C. S. et al. K-ras mutations and benefit from cetuximab in advanced colorectal cancer. *N. Engl. J. Med.* **359**, 1757–1765 (2008).
4. Camps, M., Nichols, A. & Arkinstall, S. Dual specificity phosphatases: a gene family for control of MAP kinase function. *FASEB J.* **14**, 6–16 (2000).
5. Caunt, C. J. & Keyse, S. M. Dual-specificity MAP kinase phosphatases (MKPs): shaping the outcome of MAP kinase signalling. *FEBS J.* **280**, 489–504 (2013).
6. Low, H. B. & Zhang, Y. Regulatory roles of MAPK phosphatases in cancer. *Immune Netw.* **16**, 85–98 (2016).
7. Muda, M. et al. MKP-3, a novel cytosolic protein-tyrosine phosphatase that exemplifies a new class of mitogen-activated protein kinase phosphatase. *J. Biol. Chem.* **271**, 4319–4326 (1996).
8. Moncho-Amor, V. et al. Role of Dusp6 phosphatase as a tumor suppressor in non-small cell lung cancer. *Int. J. Mol. Sci.* **20**, 2036 (2019).
9. Wong, V. C. et al. Tumor suppressor dual-specificity phosphatase 6 (DUSP6) impairs cell invasion and epithelial-mesenchymal transition (EMT)-associated phenotype. *Int. J. Cancer* **130**, 83–95 (2012).
10. Wittig-Blaich, S. et al. Systematic screening of isogenic cancer cells identifies DUSP6 as context-specific synthetic lethal target in melanoma. *Oncotarget* **8**, 23760–23774 (2017).
11. Lv, C. et al. The function of BTG3 in colorectal cancer cells and its possible signaling pathway. *J. Cancer Res. Clin. Oncol.* **144**, 295–308 (2018).
12. Bagnyukova, T. V. et al. DUSP6 regulates drug sensitivity by modulating DNA damage response. *Br. J. Cancer* **109**, 1063–1071 (2013).
13. Gao, Y. et al. Overexpression of DUSP6 enhances chemotherapy-resistance of ovarian epithelial cancer by regulating the ERK signaling pathway. *J. Cancer* **11**, 3151–3164 (2020).
14. Messina, S. et al. Dual-specificity phosphatase DUSP6 has tumor-promoting properties in human glioblastomas. *Oncogene* **30**, 3813–3820 (2011).
15. Cheng, Y. et al. PKN2 in colon cancer cells inhibits M2 phenotype polarization of tumor-associated macrophages via regulating DUSP6-Erk1/2 pathway. *Mol. Cancer* **17**, 13 (2018).
16. Li, C. et al. Excess PLAC8 promotes an unconventional ERK2-dependent EMT in colon cancer. *J. Clin. Invest.* **124**, 2172–2187 (2014).
17. Zeng, K. et al. LRIG3 represses cell motility by inhibiting slug via inactivating ERK signaling in human colorectal cancer. *IUBMB Life* **72**, 1393–1403 (2020).
18. Lee, H. J., Kim, M. Y. & Park, H. S. Phosphorylation-dependent regulation of Notch1 signaling: the fulcrum of Notch1 signaling. *BMB Rep.* **48**, 431–437 (2015).

19. Aster, J. C., Pear, W. S. & Blacklow, S. C. The varied roles of Notch in cancer. *Annu. Rev. Pathol.* **12**, 245–275 (2017).
20. Gharaibeh, L., Elmadany, N., Alwosaibai, K. & Alshaer, W. Notch1 in cancer therapy: possible clinical implications and challenges. *Mol. Pharmacol.* **98**, 559–576 (2020).
21. Arcaroli, J. J. et al. A NOTCH1 gene copy number gain is a prognostic indicator of worse survival and a predictive biomarker to a Notch1 targeting antibody in colorectal cancer. *Int. J. Cancer* **138**, 195–205 (2016).
22. Mohamed, S. Y. et al. The prognostic value of cancer stem cell markers (Notch1, ALDH1, and CD44) in primary colorectal carcinoma. *J. Gastrointest. Cancer* **50**, 824–837 (2019).
23. Fender, A. W., Nutter, J. M., Fitzgerald, T. L., Bertrand, F. E. & Sigounas, G. Notch-1 promotes stemness and epithelial to mesenchymal transition in colorectal cancer. *J. Cell Biochem.* **116**, 2517–2527 (2015).
24. Arkell, R. S. et al. DUSP6/MKP-3 inactivates ERK1/2 but fails to bind and inactivate ERK5. *Cell Signal* **20**, 836–843 (2008).
25. Katoh, M. & Katoh, M. Precision medicine for human cancers with Notch signaling dysregulation (Review). *Int. J. Mol. Med.* **45**, 279–297 (2020).
26. Klijn, C. et al. A comprehensive transcriptional portrait of human cancer cell lines. *Nat. Biotechnol.* **33**, 306–312 (2015).
27. Tung, Y. T. et al. Presenilin-1 regulates the expression of p62 to govern p62-dependent tau degradation. *Mol. Neurobiol.* **49**, 10–27 (2014).
28. Neufert, C., Becker, C. & Neurath, M. F. An inducible mouse model of colon carcinogenesis for the analysis of sporadic and inflammation-driven tumor progression. *Nat. Protoc.* **2**, 1998–2004 (2007).
29. Vinson, K. E., George, D. C., Fender, A. W., Bertrand, F. E. & Sigounas, G. The Notch pathway in colorectal cancer. *Int. J. Cancer* **138**, 1835–1842 (2016).
30. Morrugares, R. et al. Phosphorylation-dependent regulation of the NOTCH1 intracellular domain by dual-specificity tyrosine-regulated kinase 2. *Cell Mol. Life Sci.* **77**, 2621–2639 (2020).
31. Vasileva, M. V., Khromova, N. V., Kopnin, B. P., Dugina, V. B. & Kopnin, P. B. Significance of NOTCH1 expression in the progression of human lung and colorectal cancers. *Biochemistry* **87**, 1199–1205 (2022).
32. Fryer, C. J., White, J. B. & Jones, K. A. Mastermind recruits CycC:CDK8 to phosphorylate the Notch ICD and coordinate activation with turnover. *Mol Cell* **16**, 509–520 (2004).
33. Ann, E. J. et al. Tumor suppressor HIPK2 regulates malignant growth via phosphorylation of Notch1. *Cancer Res.* **76**, 4728–4740 (2016).
34. Maillet, M. et al. DUSP6 (MKP3) null mice show enhanced ERK1/2 phosphorylation at baseline and increased myocyte proliferation in the heart affecting disease susceptibility. *J. Biol. Chem.* **283**, 31246–31255 (2008).
35. Beaudry, K. et al. Dual-specificity phosphatase 6 deletion protects the colonic epithelium against inflammation and promotes both proliferation and tumorigenesis. *J. Cell Physiol.* **234**, 6731–6745 (2019).
36. Bermudez, O. et al. Post-transcriptional regulation of the DUSP6/MKP-3 phosphatase by MEK/ERK signaling and hypoxia. *J. Cell Physiol.* **226**, 276–284 (2011).
37. Fortelny, N., Overall, C. M., Pavlidis, P. & Freue, G. V. C. Can we predict protein from mRNA levels? *Nature* **547**, E19–E20 (2017).
38. Wu, Q. N. et al. Pharmacological inhibition of DUSP6 suppresses gastric cancer growth and metastasis and overcomes cisplatin resistance. *Cancer Lett.* **412**, 243–255 (2018).
39. Ye, Q., Cai, W., Zheng, Y., Evers, B. M. & She, Q. B. ERK and AKT signaling cooperate to translationally regulate survivin expression for metastatic progression of colorectal cancer. *Oncogene* **33**, 1828–1839 (2014).
40. Falco, A. et al. BAG3 controls angiogenesis through regulation of ERK phosphorylation. *Oncogene* **31**, 5153–5161 (2012).
41. Sears, R. et al. Multiple Ras-dependent phosphorylation pathways regulate Myc protein stability. *Genes Dev.* **14**, 2501–2514 (2000).
42. Tung, Y. T. et al. Sodium selenite inhibits gamma-secretase activity through activation of ERK. *Neurosci. Lett.* **440**, 38–43 (2008).
43. Ledo, J. H. et al. Presenilin 1 phosphorylation regulates amyloid-beta degradation by microglia. *Mol. Psychiatry* **26**, 5620–5635 (2021).
44. Matz, A. et al. Identification of new Presenilin-1 phosphosites: implication for gamma-secretase activity and Abeta production. *J. Neurochem.* **133**, 409–421 (2015).
45. Kim, S. K. et al. ERK1/2 is an endogenous negative regulator of the gamma-secretase activity. *FASEB J.* **20**, 157–159 (2006).
46. Hornbeck, P. V. et al. PhosphoSitePlus, 2014: mutations, PTMs and recalibrations. *Nucleic Acids Res.* **43**, D512–D520 (2015).
47. Xu, H. et al. Dual specificity MAPK phosphatase 3 activates PEPCK gene transcription and increases gluconeogenesis in rat hepatoma cells. *J. Biol. Chem.* **280**, 36013–36018 (2005).
48. Wu, Z. et al. MAPK phosphatase-3 promotes hepatic gluconeogenesis through dephosphorylation of forkhead box O1 in mice. *J. Clin. Invest.* **120**, 3901–3911 (2010).
49. Pajvani, U. B. et al. Inhibition of Notch signaling ameliorates insulin resistance in a FoxO1-dependent manner. *Nat. Med.* **17**, 961–967 (2011).
50. Png, C. W. et al. DUSP10 regulates intestinal epithelial cell growth and colorectal tumorigenesis. *Oncogene* **35**, 206–217 (2016).

Acknowledgements

This work was supported by grants from the National University Health System of Singapore (NUHSRO/2021/110/T1/Seed-Sep/03 to C.W.P.), and the Singapore National Medical Research Council (NMRC/OFIRG22jul-0061 to Y.Z.).

Author contributions

Conceptualisation: C.W.P. and Y.Z; Methodology: C.W.P., M.W., H.L., S.Z., R.M.S. and Y.Z.; Patient samples acquisition: C.S.C., K.K.T., C.W.P. and Y.Z.; Data acquisition and analysis: C.W.P., M.W., H.L., X.H., F.Y.T., S.H., S.Z., F.Y.K.W., M.R., G.C., R.M.S. and Y.Z.; Writing original draft and revisions: C.W.P., M.W., H.L., S.Z., R.M.S. and Y.L.Z.

Competing interests

The authors declare no competing interests.

Additional information

Supplementary information The online version contains supplementary material available at https://doi.org/10.1038/s41467-024-54383-y.

Correspondence and requests for materials should be addressed to Yongliang Zhang.

Peer review information *Nature Communications* thanks Rene Jackstadt and the other anonymous reviewer(s) for their contribution to the peer review of this work. A peer review file is available.